World Conference on Timber Engineering Oslo 2023

YIELD MECHANISM OF PERFORATED PLATE CONNECTIONS FOR MASS TIMBER SYSTEMS

Hossein Daneshvar [1], Thomas Tannert [2], Ying He Chui [3], Carla Dickof [4]

ABSTRACT: Mechanical connections are often the only source of ductile behaviour in mass-timber systems. This paper presents an experimental study on using perforated steel plates as a dissipating energy device, also called a seismic fuse, to enhance the structural performance of mass timber systems during extreme loading events. A target application of the perforated plate connection is in braced timber frames. Six perforation patterns were developed based on preceding experimental and numerical studies and tested under cyclic loads. These different patterns targeting one or multiple yielding mechanisms: shear, axial (tension and compression), and bending. The hysteresis performance and failure mechanism of the perforated plate systems showed that the selected patterns provided reliable yield mechanisms and that damage to timber elements can be avoided when the fuses are combined with capacity-protected dowel-type fasteners. In addition, the results of cyclic tests demonstrated sufficient ductility and ultimate displacement for specific patterns, e.g., specimens with long oval perforations, to achieve the desired energy dissipation.

KEYWORDS: Braced Timber Frame, Ductile Connections, Structural Fuse, Perforated Steel Plate, Seismic Force Resisting System

1 INTRODUCTION

The design of tall timber buildings in high seismic regions is still a challenge, mainly due to the limited energy dissipating systems and/or connections with high-performance and established practical design procedures for seismic force resisting system (SFRS). Due to the inherent brittleness of wood, other ductile materials, such as steel, are used to provide the ductility required in a seismic event. Conventionally, metal dowel-type fasteners, e.g., nails, drift pins, screws, or bolts, are a common source of ductility in timber structures. However, due to the damage they may cause to the timber components, it is beneficial to localize damage in a certain part of the structure, called seismic fuses, that are replaceable after a seismic event, with little damage to the rest of the structural system. Perforated plates are categorized as a "yielding damper" in which kinetic energy due to seismic motions is dissipated through the yielding of the steel component. In steel frames, the perforated plate fuse concept has been shown to be successful as documented in previous studies [1-8].

Specific to timber structures, Zhang et al. [9] applied glued-in, perforated plates in hold-down connections. Focusing on a specific perforation pattern confirmed their predictive ability and scalability when shear yielding was dominant. Blomgren et al. [10] and Morrell et al. [11] used a specific perforated pattern in panel-to-panel connections in cross-laminated timber shear walls. Dires and Tannert [12] extended the work on such fuses by using the concept of internal panel-to-panel connections and hold-downs. Daneshvar et al. used perforated plate fuses to panel-to-panel connections [13] and base shear connections [14] in shear walls, as well as to end brace connections in braced timber frames (BTF). They developed an analytical model for strength and prediction of ultimate deformation, verified by limited test results on specific perforation patterns. An example of such fuses at the end of a glulam brace member is shown in Figure 1.

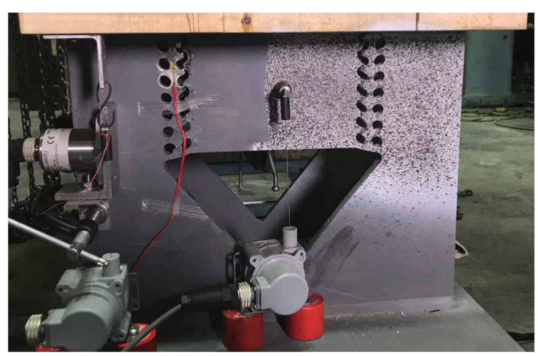

Figure 1: *Shear yielding circular perforations used in end brace connections of BTF as a seismic fuse*

[1] Hossein Daneshvar, University of Alberta, Canada, Hossein.daneshvar@ualberta.ca
[2] Thomas Tannert, University of Northern British Columbia, Canada, thomas.tannert@unbc.ca
[3] Ying-Hei Chui, University of Alberta, Canada, yhc@ualberta.ca
[4] Carla Dickof, Fast + Epp, Canada, cdickof@fastepp.com

https://doi.org/10.52202/069179-0273

Figure 1 showcases an example of shear yielding of a 12 mm thick plate with a 10 mm diameter circular perforation with a centre-to-centre spacing of 25 mm. The "link" element, defined as the minimum clear distance between two adjacent perforations, dictates the behaviour of the connection. Previous studies confirmed that the characteristic behaviour of the link elements could reasonably predict the behaviour of the connection system made of perforated plates [9, 13, 14]. However, despite adequate ductility being achieved under monotonic loading, the corresponding ductility under cyclic loading was substantially decreased, necessitating further investigation.

2 EXPERIMENTAL PROGRAM

2.1 OBJECTIVE

Based on the findings from previous research [9, 13, 14], it was postulated that the reduced ductility under cyclic loading was related to the onset of shear yield failure of the link elements between circular holes. An additional test program was deemed necessary to investigate perforation patterns to achieve flexural and axial yielding of the perforation, as opposed to the shear yielding in the earlier experimental phase. The main goal is to enhance the response of the connections in the cyclic behaviour, increasing the ductility and ultimate displacement the specimens can endure by delaying the fatigue-type failure initiations in the link elements.

2.2 FUSE PATTERNS

Six perforation patterns, as listed in Table 1, were designed and subsequently tested at the UNBC Wood Innovation Research Laboratory in Prince George, Canada. A total of twelve end brace connection specimens were tested using Method C of ASTM E2126 [15]. When the specimens were loaded by an axial force, the stress fields around the perforation zones could be in shear, axial, flexural, or a combination thereof, depending on the perforation shape and pattern. The perforation details for the oval patterns are shown in Figure 2 as a sample.

Table 1: *Fuse types tested*

Type	Fuse Pattern[1]	Specimen code
1	Oval	EBC-O
2	Circular Staggered	EBC-S
3	Circular Staggered – Buckling Restrained	EBC-BR
4	Oval Staggered (Modified)	EBC-OS[2]
5	Long Oval	EBC-LO
6	Smooth Diamond	EBC-SD

[1] Each specimen had two replicas, resulting in twelve total tests labelled, e.g., EBC-O-1 and EBC-O-2.

[2] EBC-OS-1 and EBC-OS-2 had a minor difference, c.f. section 3.4.

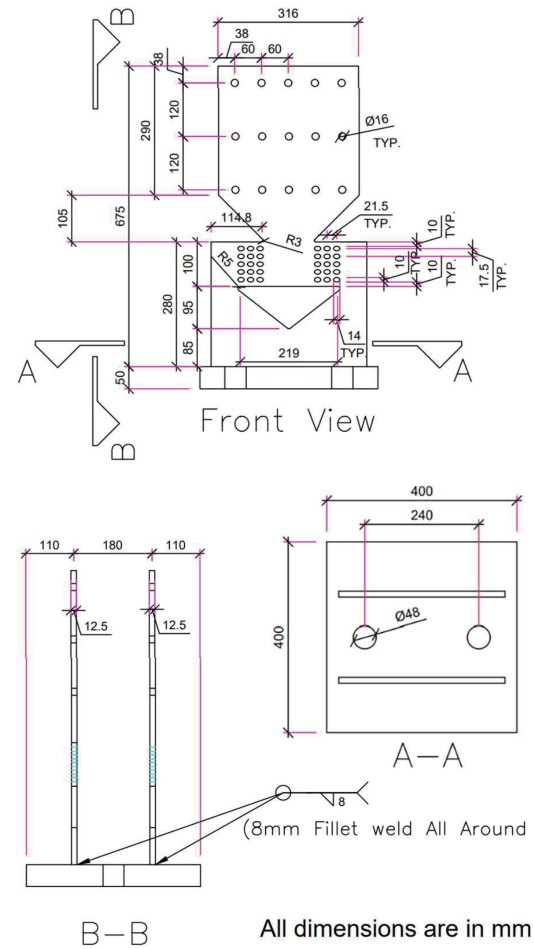

Figure 2: *Sample fuse end for EBC-O*

2.3 MATERIALS, METHOD, AND INSTRUMENTATION

The perforated plate fuses were applied to end brace connections in BTF. However, it can be noted that the perforation patterns can also be utilized in other timber SFRS, such as CLT shear walls. The timber member was 1.1 m long, 365 mm x 380 mm spruce-pine glulam grade 12c-E according to CSA O86 [16].

As shown in Figure 3 (a), the specimens consisted of fuses and capacity-protected dowel-type connections at one end (bottom) and capacity-protected connection at the other end (top). Fifteen and twenty tight-fit steel dowels of diameter 16 mm were used in the capacity-protected and fuse end connections, respectively. The specimens were instrumented using six Linear Variable Differential Transformers (LVDT), as shown in Figure 3 (b), labelled LVDT1 to LVDT6. The average displacement of the perforation zones was recorded by LVDT1 and LVDT2 . LVDT3 to LVDT6 were used to monitor the deformation in the capacity-protected steel dowels.

(a)

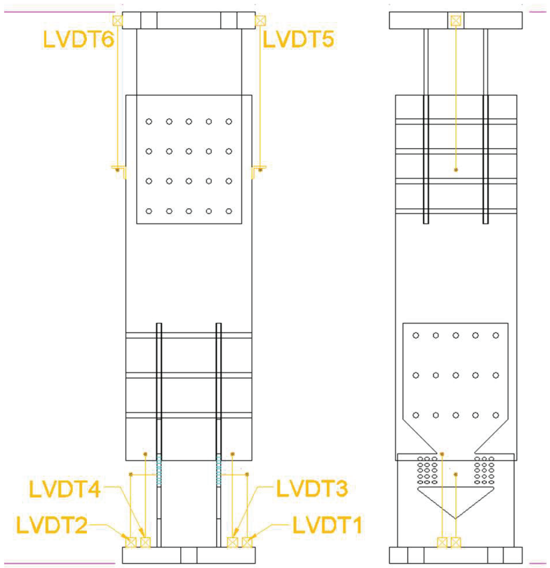

(b)

Figure 3: *Sample specimen: (a) photo, (b) schematic, instrumentation included*

3 RESULTS

The deformed shape and its corresponding load-deformation hysteresis curves for selected specimens are shown in Figures 4 and 5, respectively. Detailed analysis of the test results is currently in progress at the time of writing this paper. Some preliminary findings and test observations are presented below.

3.1 EBC-O

The signs of yielding in all the link elements, both horizontal and vertical, were obvious before failure initiation. It is not easy to distinguish if the yielding of links is flexural or shear; however, considering the link elements' aspect ratio, it seems reasonable to assume shear-flexural yielding. The failure is initiated with a sudden rupture of inner link elements and propagates vertically to other elements in the row. Almost the same failure mode was observed in both replicates; the failure mode of EBC-O-2 is shown in Figure 5 (a). The other rows, while uniformly yielded, did not experience any rupture. Both specimens achieved similar ultimate displacements but different peak loads. The hysteresis curve of EBC-O-2 is shown in Figure 6 (a). As can be seen, the curve is wide, with substantial energy dissipation capability.

3.2 EBC-S

Due to a mistake in load application, EBC-S-1 was subjected to a monotonic load and buckled. EBC-S-2 was loaded cyclically, as anticipated; but similarly failed due to the global buckling of the knife plates, as shown in Figure 5 (b). The weak line was found where the perforation ends, and the triangular cut-out is maximized. While global buckling of the plates could be used as a source of energy dissipation, the difference in tensile and compressive responses, as noted in Figure 6 (b), might make it difficult to predict the onset of yielding. The pinching behaviour due to the buckling of the plate in compression is evident. Pattern EBC-S was initially aimed at achieving axial yielding in the perforation zones. The observed buckling behaviour necessitated modifying the perforation patterns to achieve the target failure mode. This led to the buckling restrained specimens of EBC-BR, as discussed below, in 3.3.

3.3 EBC-BR

EBC-BR contains a larger perforation diameter compared to EBC-S. In addition, four stiff plates were welded to the outer sides of the knife plates. The failure mode of EBC-BR-2 is shown in Figure 5 (c). As can be seen, these two major changes caused the shift in failure mode from global plate buckling to axial yielding of link elements, as intended. The link on the inner rows is mainly ruptured due to excessive yielding, while there were no ruptures observed in other rows, although significant yielding was observed. Figure 6 (c) depicts that this fuse pattern possesses ample wide hysteresis curves, with improved strength and ultimate displacement, compared with EBC-S.

3.4 EBC-OS

EBC-OS-1, similar to EBC-S-1 and EBC-S-2, globally buckled at the weak line of the minimum cross section. Increasing the size of perforations in EBC-OS-2 shifted the failure mode from global buckling to rupture in the perforation zones, as seen in Figure 5 (d). The intended axial yielding mechanism is achieved in the EBC-OS-2. Also, the pinching observed due to buckling in the hysteresis loops of the EBC-OS-1 faded away in the EBC-OS-2 responses, as shown in Figure 6 (d). The larger perforations also allow an increase in ultimate displacement achieved by the specimen.

 https://doi.org/10.52202/069179-0273

(a)

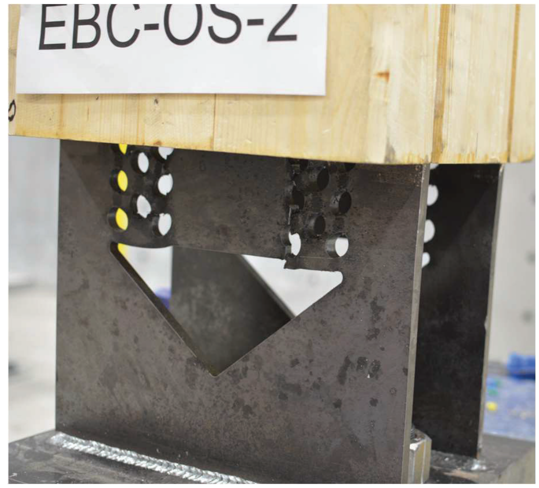

(d)

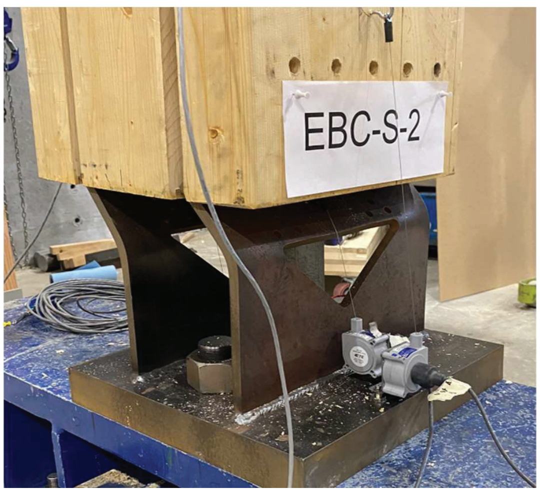

(b)

(e)

(c)

(f)

Figure 4: *Failure modes and deformed shapes*

https://doi.org/10.52202/069179-0273

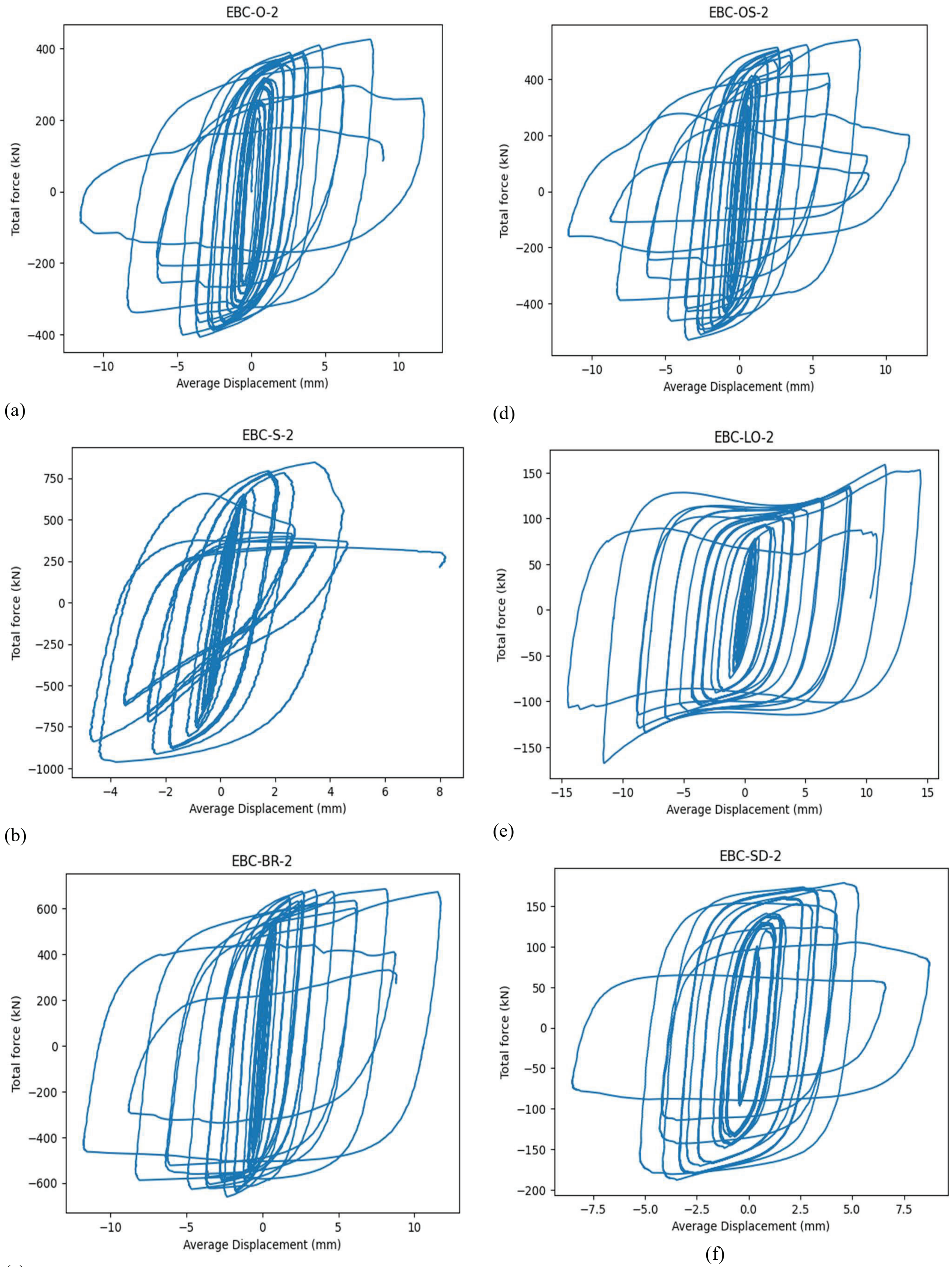

Figure 5: *Hysteresis curves*

https://doi.org/10.52202/069179-0273

3.5 EBC-LO

The target failure mode for this pattern was flexural yielding, achieved by forming two plastic hinges at the ends of link elements. The two specimens behaved almost the same. Figure 5 (e) shows the failure mode of EBC-LO-2); the outer plastic hinges experienced rupture first in the majority of perforation zones, and then the failure propagated to the inner plastic hinges of the link elements. The hysteresis loops of the two specimens were almost the same; see Figure 6 (e) corresponding to EBC-LO-2, for instance. The results show reasonable ductility for the fuses, with large open hysteretic loops reflecting the ability of the fuse to dissipate energy. Significant ultimate displacements were observed with this pattern compared with other patterns, suggesting that the flexural mechanism, achieved with the long oval-shaped perforations, could be the desired pattern to improve the fuse behaviour under cyclic loading.

3.6 EBC-SD

Like EBC-LO specimens, the intended yielding mechanism for EBC-SD specimens was also flexural yielding. However, instead of two plastic hinges at the ends of the link elements, a non-prismatic cross section was used to force the formation of the plastic hinges in the middle of the link elements. The intended failure mode was achieved in both specimens; Figure 5 (f) shows the EBC-LO-1 failure mode. Although the hysteresis loops are wider compared to the EBC-LO pattern, limited ultimate displacement caused the dissipative energy capability of the fuse to be insignificant, see Figure 6 (f). However, the hysteresis behaviour of the fuse, in terms of the area enclosed per cycle, looks promising and may be enhanced with minor revisions in the future.

3.7 FUSE REPLACEABILITY

As illustrated in Figure 7, all damage was concentrated in the perforation zones . The capacity-protected steel dowel connections were undamaged and could be disassembled. The fuse end connection can be easily removed after the cyclic tests, representing the resiliency of the fuse with no damage to the timber component. To reliably design capacity-protected dowel-type connections, research to quantify the over-strength factor is ongoing.

4 CONCLUSIONS

Under cyclic loading, twelve full-scale end brace connection specimens with six different steel plate perforation patterns were tested. These perforated plates, developed based on preceding experimental and numerical studies, were intended to be seismic fuses. The triggered yielding mechanisms were shear, axial, flexural, or a combination. Long oval perforations provided the best performance regarding ductility, energy dissipation, and ultimate displacement. The evaluated perforated plate patterns provided resilient solutions that could be replaced after yielding failure.

Figure 6: *Resiliency in terms of replaceability*

ACKNOWLEDGEMENT

The authors would like to acknowledge the financial support of the Natural Sciences and Engineering Research Council of Canada (NSERC) through the Industrial Research Chair program as well as the Natural Resources Canada (NRCan) through the Green Construction through Wood (GCWood) program—special thanks to Western Archrib for supplying the glulam members. The support by the UNBC technicians Michael Billups, James Andal, and Ryan Stern is greatly appreciated.

REFERENCES

[1] Eatherton, M., Hajjar, J., Deierlein, G., Krawinkler, H., Billington, S. and Ma, X. Controlled Rocking of Steel-framed Buildings with Replaceable Energy-dissipating Fuses. *Proceedings of the 14th World Conference on Earthquake Engineering*, Beijing, China, 2008.

[2] Ma, X. Seismic Design and Behavior of Self-centering Braced Frame with Controlled Rocking and Energy Dissipating Fuses. Ph.D. thesis, Stanford University, Stanford, California, United States, 2011.

[3] Kobori, T. Miura, Y. Fukuzawa, E., Yamada, T., Arita, T., Takenake, Y. and Fukumoto, T. Development and Application of Hysteresis Steel Dampers. *Proceedings of the 10th World Conference on Earthquake Engineering*, Rotterdam, Netherlands, 2341-2346, 1992.

[4] Chan, R.W.K. and F. Albermani. Experimental Study of Steel Slit Damper for Passive Energy Dissipation. Engineering Structures, 30(4): 1058-1066, 2008.

[5] Teruna, D., Majid, T. and Budiono, B. Experimental Study of Hysteretic Steel Damper for Energy Dissipation Capacity. Article ID 631726, *Advances in Civil Engineering,* 2015.

[6] Lee, C.L., Ju, Y.K., Min, J.K., Lho, S.H. and Kim, S.D. Non-uniform Steel Strip Dampers Subjected to Cyclic Loadings. Engineering Structures, 99: 192-204, 2015.

[7] Ahmadie Amiri, H. Najafabadi, E. and Estekanchi, H. Experimental and Analytical Study of Block Slit Damper. Journal of Constructional Steel Research, 141: 167-178, 2018.

[8] Li, T. Experimental Testing and Numerical Modelling of Honeycomb Structural Fuse. MASc thesis, Department of Civil Engineering, University of British Columbia, Vancouver, British Columbia, Canada, 2018.

[9] Zhang, X., Popovski, M., and Tannert, T. High-capacity hold-down for mass-timber buildings. Construction and Building Materials, 164: pp. 688-703, 2018.

[10] Blomgren, H.-E. Pei, S. Powers, J. Dolan, J. Wilson, A. and Jin, Z. Cross-laminated Timber Rocking Wall with Replaceable Fuses: Validation through Full-scale Shake Table Testing. *Proceedings of WCTE 2018: World Conference on Timber Engineering*. Seoul, Republic of Korea, 2018.

[11] Morrell, I., Phillips, A. Dolan, J. and Blomgren, H.-E. Development of an Inter-panel Connector for Cross-laminated Timber Rocking Walls. *Proceedings of WCTE 2018: World Conference on Timber Engineering*, Seoul, South Korea, 2018.

[12] Dires, S. and Tannert, T. Performance of coupled CLT shear walls with internal perforated steel plates as vertical joints and hold-downs. Journal of Construction and Building Materials, 346(3): 128389, 2022.

[13] Daneshvar, H., Niederwestberg, J., Dickof, C., Jackson, R. and Chui, Y.H. Perforated Steel Structural Fuses in Mass Timber Lateral Load Resisting Systems. Engineering Structures, 257: 114097, 2022.

[14] Daneshvar, H., Niederwestberg, J., Letarte, JP., and Chui, Y.H. Yield Mechanism of Base Shear Connections for Cross-Laminated Timber Shear Walls. Journal of Construction and Building Materials, 335: 127498, 2022.

[15] ASTM E2126, Standard Test Methods for Cyclic (Reversed) Load Test for Shear Resistance of Vertical Elements of the Lateral Force Resisting Systems for Buildings. ASTM International, West Conshohocken, PA, 2018.

[16] Canadian Standards Association (CSA): Engineering Design in Wood. CSA Standard 086-19. Toronto, ON, Canada, 2019.

https://doi.org/10.52202/069179-0273